PERIÓDICO TCHÊ QUÍMICA
ARTIGO ORIGINAL

EFEITO DO SELÊNIO NA ESTRUTURA SUPRAMOLECULAR E CARACTERÍSTICAS TÉRMICAS DA FIBROÍNA BOMBYX MORI L

THE EFFECT OF SELENIUM ON THE SUPRAMOLECULAR STRUCTURE AND THERMAL CHARACTERISTICS OF FIBROIN BOMBYX MORI L

ЭФФЕКТ СЕЛЕНА НА НАДМОЛЕКУЛЯРНОЙ СТРУКТУРЕ И ТЕПЛОВЫЕ ХАРАКТЕРИСТИКИ ФИБРОИН BOMBYX MORI L

SHUKURLU, Yusif H.*;

[1] Sheki Regional Scientific Center of the National Academy of Sciences of the Republic of Azerbaijan, 24 L. Abdullayev Str., zip code AZ 5500, Sheki – Azerbaijan Republic

** Correspondence author*
e-mail: yusifsh@hotmail.com

Received 12 December 2019; received in revised form 20 February 2020; accepted 08 March 2020

RESUMO

O enriquecimento da estrutura molecular da fibroína da seda pelo átomo de selênio levou a um aumento na ramificação da macromolécula da fibroína. Como resultado, a fração amorfa da microfibra da fibroína aumenta, o que leva a um aumento nas características de resistência do fio da seda. Ao mesmo tempo, essa mudança na estrutura supramolecular da fibroína envolvendo o átomo do selênio nos permitiu estudar o mecanismo de duas modificações para cristalização de microfibras da fibroína. Com base em estudos sobre o uso da análise gravimétrica térmica e análise de estrutura de raios X e as alterações relativas na proporção de regiões amorfas e cristalinas, chegamos à conclusão de que as microfibrilas da fibroína consistem principalmente em cristalitos com cadeias crescentes. Alternam-se ao longo do eixo da microfibra com camadas amorfas, cujos tamanhos são menores que os tamanhos de cristalitos dobrados. Portanto, os cristalito dobrado não pode ser localizado em camadas amorfas entre os cristalitos com cadeias crescentes ao longo do eixo da microfibra. Como resultado, a capacidade de dobrar seções ramificadas da macromolécula diminui, isto é, o CFC diminui. Isso aumenta a proporção de microfibras amorfas na fibroína. No modelo proposto pelos autores, segmentos da macromolécula não cristalizada na forma de cristalito com cadeias crescentes, localizada nas laterais do núcleo central e anexada a ele, restauram sua estrutura dobrada – na forma de dobras de uma placa de cristalitos.

Palavras-chave: *biodegradabilidade, domínios cristalinos, folha beta de Pauling-Corey, polímero, fios adjacentes.*

ABSTRACT

The enrichment of the molecular structure of silk fibroin by selenium atom led to an increase in the branching of fibroin macromolecule. As a result, the amorphous fraction of fibroin microfiber increases which leads to an increase in the strength characteristic of the silk thread. At the same time, this change in the supramolecular structure of fibroin involving a selenium atom has enabled us to study the two-modification mechanism for crystallizing fibroin microfibers. Based on studies on the use of temperature-gravimetric and X-ray diffraction (XRD) analysis and relative changes in the proportion of amorphous and crystalline regions, we came to the conclusion that fibroin microfibrils consist mainly of extended crystallites CSC – crystallites with the stretched chains. They alternate along the axis of microfiber with amorphous layers, the sizes of which are smaller than the sizes of the folded crystallites (CFC). Therefore, CFC cannot be located in amorphous layers between the CSC along the microfiber's axis. As a result, the ability to fold branched sections of the macromolecule decreases, that is, CFC decreases. This increases the proportion of amorphous areas of microfibers of the fibroin. In the model, which is proposed by author non-crystallized in the form of CSC, segments of a macromolecule, on the sides of the central core and attached to it, restored their crystal structure (CFC) – with folded conformation of chains.

Keywords: *silk fibroin microfibers, selenium enrichment, Pauling-Corey beta-sheet, biopolymer, crystallization with "shish-kebab" morphology, adjacent filaments*.

DOI: 10.52571/PTQ.v17.n34.2020.615_P34_pgs_591_598.pdf

АННОТАЦИЯ

Обогащение молекулярной структуры фиброина шелка атомом селена привело к увеличению разветвленности макромолекулы фиброина. В результате аморфная фракция микроволокна фиброина увеличивается, что приводит к увеличению прочностных характеристик шелковой нити. В то же время это изменение надмолекулярной структуры фиброина с участием атома селена позволило нам изучить механизм двух модификаций для кристаллизации фиброиновых микроволокон. Основываясь на исследованиях по использованию температурно-гравиметрического и рентгеноструктурного анализа (РСА) и относительных изменений в пропорции аморфных и кристаллических областей, мы пришли к выводу, что фиброиновые микрофибриллы состоят в основном из протяженных кристаллитов КРЦ – кристаллитов с растянутыми цепями. Они чередуются вдоль оси микрофибры с аморфными слоями, размеры которых меньше размеров складчатых кристаллитов (КСЦ). Следовательно, КСЦ не может быть расположен в аморфных слоях между КРЦ вдоль оси микрофибры. В результате уменьшается способность складывать разветвленные участки макромолекулы, то есть снижается количество КРЦ. Это увеличивает долю аморфных участков микроволокон в фиброине. В модели, которая предложена авторам, некристаллизованные в виде КРЦ, сегменты макромолекулы, расположенные по бокам центрального ядра и прикрепленные к нему, восстанавливают их кристаллическую структуру (КСЦ) – при сложенной конформации цепей.

Ключевые слова: *микрофибрлл фиброина шелка, разветвление селеном, бета-лист Полинга-Кори, полимер, кристаллизация с морфологией «шашлык», смежные нити*.

1. INTRODUCTION

At present, it has become possible to use silk fiber waste (SW) for the development of silk fibroin (SF) films that exhibit differentiated behavior in terms of biodegradability, mechanical strength, and other specific properties (Jaramillo-Quiceno *et al.*, 2017). The authors of (He *et al.*, 1999), are using new technology – foaming. Bombyx mori SF single crystals are obtained in metastable polymorph of silk I. They found that weak acidic conditions in the solution from which the foam was obtained contribute to the formation of silk II, while neutral to weak basic solutions contribute to the formation of silk I. During foaming, more dilute solutions contribute to the formation of silk II while more concentrated solutions (about 7 wt.% or more) contribute to the formation of silk I.

The author of (Fossey *et al.*, 1991) proposed a new model structure for the form of silk I, the crystalline domains of fibroin of silk Bombyx mori and also for the corresponding crystalline form of poly (L-Ala-Gly), which make up the structure of silk II. The main difference between the two structures is the orientation of the side chains of adjacent filaments in each sheet. In the Pauling-Corey beta-sheet and in the structure of silk II called the “register” structure, the Ala side chains of each strand point to the same side of the sheet. In the silk structure I, called the “off-register”, the side chains of Ala residues in adjacent strands point to opposite sides of the sheet. Thus, according to the authors, some of the secondary structures obtained in the regenerated SF materials include crystalline and amorphous structures. Since crystalline structures include the dominant conformation of β-turns (silk I) and the insoluble structure formed by folded β-sheets (silk II).

The authors of (Jaramillo-Quiceno *et al.*, 2017) estimated the presence of crystalline (silk I and silk II) and amorphous structures by using XRD and Attenuated Total Reflection and Fourier Transform Infra-Red (ATR-FTIR) spectroscopy. The thermal properties of SF films were studied by DSC. According to the FTIR and XRD results, the presence of silk structure I in SF wastes is greater than in SF cocoons. Differences in the enthalpy of crystallization peaks on DSC curves show that SF cocoons have a higher content of amorphous structures than SF wastes, etc. It is known that SF is widely used to create three-dimensional matrices that contribute to the restoration of damaged organs and tissues, biodegradable cell carriers, drugs, etc. (Agapova, 2017). In this regard, our researchers continue to thoroughly study the structural features of this biopolymer.

Thus, we present our results obtained in the study of the effect of selenium on the molecular and supramolecular structures of silk fibroin. Note that in the mid-seventies of the last century, June Magoshi and Shigeo Nakamura investigated the thermal decomposition of SF (Jun Magoshi and Nakamura, 1975). It was shown that decomposition occurs with the formation of

endothermic and exothermic peaks. They explained that the endothermic shift observed at 448K on the DSC curve (curves on the differential scanning calorimetry) was due to the glass transition. The exothermic peak at 485K was recognized by them as crystallization, which was subsequently confirmed by XRD analysis. It was shown that the endothermic peak at 553K is a decomposition of the polymer.

Comparative changes in the supramolecular structure of fibroin microfibrils, ordinary and enriched selenium atoms were studied. At the same time, we used various research methods: we studied the accumulation of free radicals during deformation and irradiation of a silk thread with a full spectrum of an ultraviolet lamp with electron- paramagnetic absorption; we used the spin probe method to determine the degree of change in the proportion of amorphous and crystalline parts of microfibrils, the combined effects and impacts of ultraviolet radiation and selenium on fibroin structure. Also, we carried out tests for deformation strength, thermomechanical and electrical strength. We used differential scanning calorimetry, X-ray diffractometry and infrared spectroscopy to study the crystalline modifications of fibroin (Abdullaev *et al.*, 1978; Abdullaev *et al.*, 1980; Bakirov *et al.*, 1981a; Bakirov *et al.*, 1981b; Shukurov (Shukurlu) *et al.*, 1981). We found that when silk fibrin is enriched with selenium, selenium atoms actively enter to the primary structure of fibroin and change the supramolecular structure, that is, it leads to a change in the relative amounts of crystalline and amorphous sections of fibroin microfibrils.

In this paper, the effect of selenium on the supramolecular structure and the quantitative change in the modification of crystallites of fibroin Bombyx mori L. are summarized.

2. MATERIALS AND METHODS

The thermophysical properties of fibroin were studied on an OD-102 system derivatograph (VNR, MOM – Paulik-Paulik-Erdey derivatograph in platinum crucibles), which uses the derivative thermogravimetry (DTG) curve and thus, makes it possible to separate the superimposing thermal effects that are inseparable neither on the differential thermal analysis (DTA) nor on the thermogravimetric (TG) curves (Kadri *et al.*, 2017). A slight change in mass which is almost not observed on the thermogravimetric curves, can easily be detected by the peaks on the DTG curve. The DTG curve allows one to quantitatively determine the fraction of individual effects since the minima – the horizontal sections of this curve – correspond to the lowest rate of change in mass, i.e., the boundary between the two effects. The thermogravimetric curve informs more accurately about the processes accompanied by a change in the mass of the test substance (Zhang *et al.*, 2017; Kostrobij *et al.*, 2018). Alumina calcined at 1270K was used as a reference. The atmosphere in the furnace is air, the initial temperature is room temperature, the heating rate is 10 deg/min, the sensitivity of the device: T (temperature) – 773K; thermogravimetric analysis (TGA) – 200; differential thermogravimetric analysis (DTGA) – 1/5; differential thermal analysis (DTA, which shares much in common with differential scanning calorimetry (DSC)) – 1/3. Weighed portions of fibroin amounted to 170mg, its crystalline part – 250mg (Shi *et al.*, 2018; Steffi *et al.*, 2018).

To assess the quantitative ratio of the two crystalline modifications and their sizes, we used DRON-2 stationary X-ray diffractometer (was released in 1978) with CuKα radiation with rectified voltage 37kV (λ = 0.154nm) which allowed us to measure the intensities of the XRD beam in a given direction and diffraction angle 2θ. The Debye-Scherrer method ("powder" method) was used for the XRD analysis of fibroin. As a sample, the powder of the crystalline part of fibroin was used.

3. RESULTS AND DISCUSSION:

The end effect on the DTA curve with a minimum of about 360K is observed for all samples and characterizes fibroin dehydration (Jun Magoshi and Nakamura, 1975; Xudayberdiyeva, 2009). The plateau with a fracture at 490K in the temperature range of 450-490K is caused by amorphous regions present in the structure, and its length for fibroin enriched with selenium (Figure 1b) is much larger than for the control (not enriched with selenium) sample (Figure 1a). This confirms the conclusion made above about the increase in the proportion of amorphous parts in experimental samples of fibroin. The exothermic peak of DTA which is about 550K (in the temperature range of 490-560K), characterizes the crystallization of molten amorphous parts of the polymer. In the initial stage of the melting of a polycrystalline substance, a two-phase state forms and the heat capacity sharply changes.

Therefore, an exothermic peak is revealed before the endo-melting effect (upon disordering). Such a peak is not clearly visible for fibroin (Figure 2), unlike its crystalline part (Figure 1). This is

probably due to the specificity of the ratio of the volume fraction of amorphous and crystalline sections of the polymer. From the very beginning of the creation of this method, specialists aimed to use DTA curves to determine quantitative ratios. Quantitative evaluations of the DTA curves were scientifically substantiated by the researchers Speil, Berkelgammer, Pask and Davis, and attempts to improve the method were reflected in the works of Kerr and Coop, Barshed, Berg, Feldvarine, Klibursky. Moreover, many researchers looked for reliable relationships between the height of the peak of the DTA curve and the content of the desired component in the sample.

Currently, the basis of the quantitative evaluation is the area bounded by the curves and the mainline. This method of quantification is correct, but it is very inaccurate and difficult. In practice, it turns out that a quantitative evaluation of DTA curves by this method can only be carried out with an accuracy not more than 5-10%. In addition, it is known that due to the DTA method, it is easy to establish the direction and magnitude of the change in enthalpy associated with chemical reactions and other processes occurring in the test substance under the influence of heat. On the other hand, by using the TGA method, it is possible to determine with high accuracy the nature and magnitude of the change in the mass of the polycrystalline sample material with an increase in temperature.

Due to the TGA curve, it is also possible to perform stoichiometric calculations or percentage calculations. Based on the listed possibilities of the mentioned methods, an idea emerged about their simultaneous use for studying the transformations in the matter that occur under the influence of elevated temperatures.

According to the TGA and DTGA curves, in the crystalline part of the fibroin enriched with selenium mass loss occurs more slowly (Figures 1b and 2b) than in the control one (not enriched with selenium) (Figures 1a and 2a). This is due to the stabilizing effect of selenium. A sharp kink is observed on the TGA curves of the crystalline part of fibroin for control samples at 570K, and on the DTA curves this is characterized by two minima at 560 and 580K. The observation of two minima for polymers in the melting region, in most cases, testifies to the presence of two types of crystallites in them – with the stretched chains (CSC) and with the folded chains (CFC) (Keller, 1967; Keller, 1968; Davidson and Wunderlich, 1969; Keller, 1975).

Based on this, it can be assumed that when a silkworm cocoon is produced, due to the influence of a filament stretch, pressure of the caterpillar spinneret, a peculiar structure of the silk-secreting part and a velocity gradient, the crystallization of fibroin occurs (an orientation process) which is accompanied by the formation of two modifications (bicomponent crystallization) – CSC and CFC.

With an increase in temperature in the chamber of a derivative gravimeter, the crystallites with elongated fibroin chains begin to break down first and after that the crystallites with folded chains. Thereby, the depth and width of the minimum DTGA of the low-temperature region corresponding to the destruction (disordering) of the CSC is much larger than the minimum of the CFC in the high-temperature region. In the case of fibroin enriched with selenium, the minimum corresponding to CFC almost disappears (Figure 2b). Therefore, when selenium is introduced into the structure of fibroin, the amount of CFC decreases, and due to this a predominant increase in the proportion of the amorphous part of the polymer occurs.

To obtain information on polymorphic crystallization, on the relative arrangement of various phases in microfibrils and their relative sizes in fibroin, we performed X-ray diffraction studies of fibroin (Shukurov (Shukurlu) *et al.*, 1981; Shukurlu, 1997). The object of the study was the crystalline part of the fibroin of the control and experimental samples. As a sample, the powder of the crystalline part of fibroin was used. In Figure 3, X-ray diffraction patterns are shown. It is seen that the intensity of the reflexes at 2θ which equal to 21.8; 24.4 and 37.2 degrees for fibroin enriched with selenium (curve 3b in Figure 3), is much less (Note that the reflex at 28.6 degrees matches with the reflection reflex of the glass cuvette of the X-ray diffractometer). In the remaining reflexes, noticeable differences are not observed. By comparing the results with thermal analysis and literature data (Lazarides, 1980; Monshi *et al.*, 2012), it can be stated that wide reflections correspond to crystallites with the stretched chains (CSC) while narrow reflections correspond to crystallites with folded chains (CFC).

Using the Scherrer formula that relates the size of small particles (crystallites) to the width of diffraction peaks, we determined only the size of crystalline particles of fibroin with an amorphous coating, such as this method is used to measure the size of polymer-coated nanoparticles (Shukurlu, 2006). As can be seen from Figure 3 the half-width of narrow reflexes is several times

smaller than that of wide reflexes (βCSC = 0.103; βCFC = 0.016). Consequently, the size of the CFC is almost ~6.5 times larger than that of the CSC (LCSC=1.366nm; LCFC = 8.821nm). It is usually believed that the integrated intensity of reflexes is directly proportional to the number of corresponding regions. According to Figure 3, the area under wide reflexes is 15 times larger than the area under narrow reflexes. Consequently, the amount of CSC is significantly (approximately 15 times) greater than that of CFC.

4. CONCLUSIONS:

Based on X-ray diffraction analysis, it was found that the size of the CFC in the microfibril is 4.2 times larger than the size of the CSC, but their number is 15 times less. When selenium is introduced into the structure of fibroin, the number and size of CSC remain constant while the number of CFC decreases by 2.5 times (according to the area of the intensity of narrow reflexes) and as a result, the proportion of amorphous sites increases by 10%.

Thus, based on the above studies, it can be concluded that fibroin microfibrils are composed mainly of CSC. They alternate along the axis of microfibrils with amorphous layers which are smaller in size than the CSC. Therefore, the CFC cannot be located in amorphous layers i.e. between the CSC along the microfibril axis. This suggests that the formation of the fibroin fiber first forms a central core of crystallites with stretched chains (CSC). With the introduction of selenium into the structure of fibroin, new lateral branches are formed in the macromolecules, which cannot enter the crystal lattice at all. As a result, the ability to fold decreases, and (due to a decrease in the number of CFCs) the proportion of amorphous sites increases. Such a model of fibroin microfibrils is presented in Figure 4. At the lateral sides of this model, the non-crystallized segments of molecules included in the central core restore their folded structure (cross-β-shape). The crystallization of such segments of fibroin macromolecules occurs in the form of CFCs with the formation of microfibrils in the form of a structure called “micro shish-kebab”.

5. REFERENCES:

1. Abdullaev, G. B., Bakirov, M. Ya., Mamedov, Sh. V., Shukurov (Shukurlu), Yu. G. *News of Azerbaijan SSR AS. Series of Physical and Technical and Mathematical Sciences*, **1980**, *2*, 86-90.
2. Abdullaev, G. B., Bakirov, M. Ya., Mamedov, Sh. V., Shukurov, (Shukurlu), Yu. G. *Scientific reports of AN Azerbaijan SSR*, **1978**, *34*(11), 20-24.
3. Agapova, O.I. *Modern technologies in medicine*, **2017**, *9*(2), 192-204.
4. Bakirov, M.Ya., Mamedov, Sh.V., Shukurov, (Shukurlu) Yu.G. *Shelk*, **1981a**, *3*, 16-17.
5. Bakirov, M.Ya., Shukurov (Shukurlu), Yu.G., Ismailova, R.S., Mamedov, Sh.V. *Shelk*, **1981b**, *4*, 27-28.
6. Davidson, T., Wunderlich, B. *Journal of Polymer Science. Part A-2: Polymer Physics*, **1969**, *7*, 2051-2059.
7. Fossey, S.A., Némethy, G., Gibson, K.D., Scheraga, H.A. *Biopolymers and Cell,* **1991**, *31*(13), 1529-1541.
8. He, S.J., Valluzzi, R., Gido, S.P. *International Journal of Biological Macromolecules*, **1999**, *24*(2-3), 187-195.
9. Jaramillo-Quiceno, N., Catalina Álvarez-López, C., Restrepo-Osorio, A. *Procedia Engineering*, **2017**, *200*, 384–388. https://doi.org/10.1016/j.proeng.2017.07.054
10. Jun Magoshi, J., Nakamura, S. *Journal of Applied Polymer Science*, **1975**, *19*(4), 1013-1015. https://doi.org/10.1002/app.1975.070190410.
11. Kadri, I., Derbel, M.A., Naïli, H., Roisnel, T., Rekik, W. *Chemical Papers*, **2017**, *71*(11), 2063-2073.
12. Keller, A. *Journal of Polymer Science: Polymer Symposia*, **1975**, *51*, 7-44.
13. Keller, A. *Reports on Progress in Physics*, **1968**, *31*, 623-705.
14. Keller, A., Machin, M. J. *Journal of Macromolecular Science*, **1967**, *B1*, 41-91.
15. Kostrobij, P., Grygorchak, I., Ivashchyshyn, F., Markovych, B., Viznovych, O., Tokarchuk, M. *Journal of Physical Chemistry A*, **2018**, *122*(16), 4099-4110.
16. Lazarides, E. *Nature*, **1980**, *283*, 249-256.
17. Monshi, A., Foroughi, M. R., Monshi, M.R. *World Journal of Nano Science and Engineering*, **2012**, *2*, 154-160. http://dx.doi.org/10.4236/wjnse.2012.23020
18. Shi, Y., Li, Z., Shi, J., Zhang, F., Zhou, X., Li, Y., Holmes, M., Zhang, W., Zou, X. *Sensors and Actuators, B: Chemical*, **2018**, *260*, 465-474.

19. Shukurlu, Yu. G. *Some features of the supramolecular structure of silk fibroin*. Sheki: Sheki Regional Scientific Center of the National Academy of Sciences of Azerbaijan. Republic, **1997**.
20. Shukurlu, Yu.G. *Structural Proteins*. Baku: Elm, **2006**.
21. Shukurov (Shukurlu), Yu.G., Kerimov, T.M., Bakirov, M.Ya., Mamedov, Sh.V. *News of Azerbaijan SSR AS. Series of Physical and Technical and Mathematical Sciences*, **1981**, *1*, 110-113.
22. Steffi, C., Wang, D., Kong, C.H., Wang, Z., Lim, P.N., Shi, Z., San Thian, E., Wang, W. *ACS Applied Materials and Interfaces*, **2018**, *10*(12), 9988-9998.
23. Xudayberdiyeva, D. B. *Textile Industry Technology*, **2009**, *2*(314), 56-61.
24. Zhang, X., Jia, C., Qiao, X., Liu, T., Sun, K. *Polymer Testing*, **2017**, *62*, 88-95.

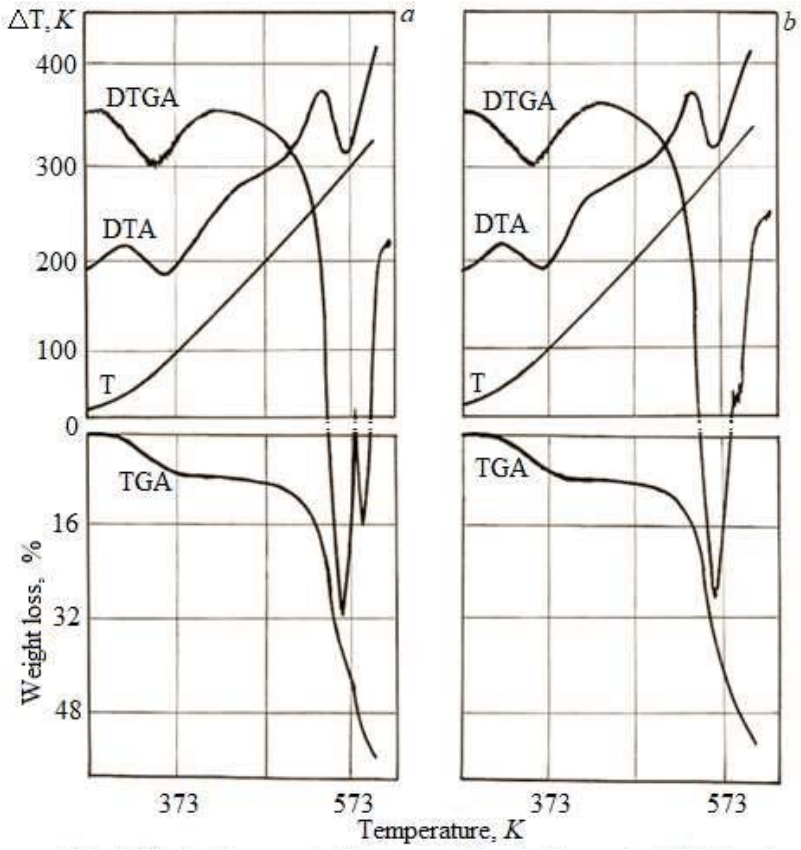

Figure 1. *Derivative gravimetric crystalline curves parts of silk fibroin: a – for control (not enriched with selenium); b – for experimental samples*

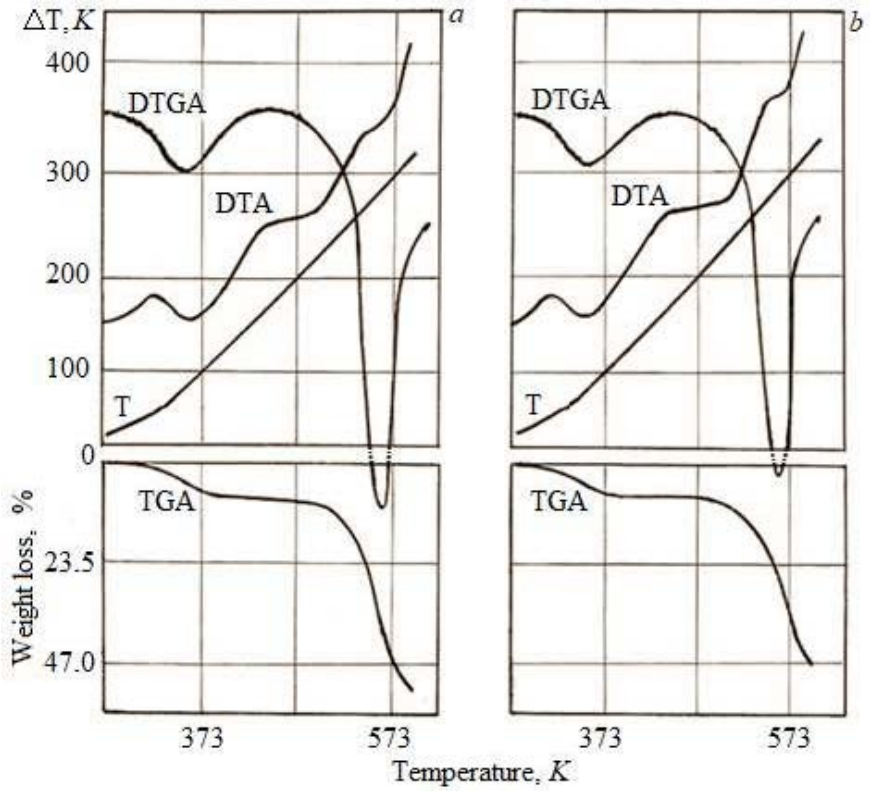

Figure 2. *Derivative gravimetric curves of silk fibroin: a – for control (not enriched with selenium); b – for experimental samples*

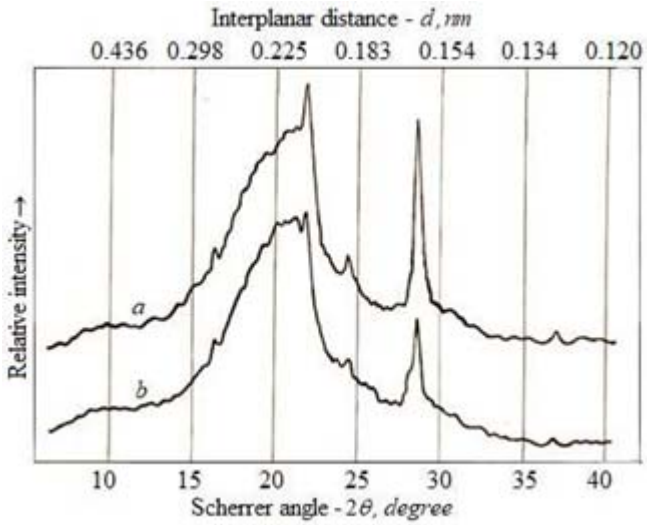

Figure 3. *X-ray diffraction patterns of silk fibroin: a – for control (not enriched with selenium); b – for experimental samples*

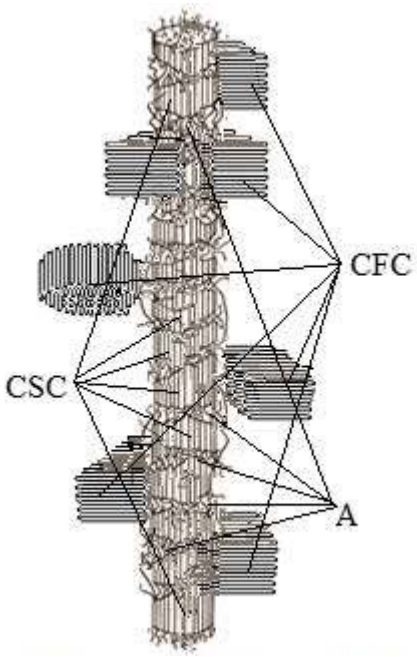

Figure 4. *Packing model of silk fibroin macromolecules forming microfibrils: CSC – crystallites with the elongated chains; CFC – crystallites with the folded chains; A – amorphous sites*